NanoWorld Journal

https://doi.org/10.17756/nwj.2023-s5-026

Research Article

Open Access

Performance Evaluation of Nanoscale Gate Engineered AlN/GaN Recessed T-gated HEMT with Fe-doped Buffer for Future Power Electronic Applications

B. Mounika, J. Ajayan and Sandip Bhattacharya*

Department of Electronics and Communications Engineering, SR University, Warangal, Telangana, India

***Correspondence to:**
Sandip Bhattacharya
Department of Electronics and Communications Engineering,
SR University,
Warangal, Telangana, India.
E-mail: 1983.sandip@gmail.com

Received: October 11, 2023
Accepted: December 19, 2023
Published: December 22, 2023

Citation: Mounika B, Ajayan J, Bhattacharya S. 2023. Performance Evaluation of Nanoscale Gate Engineered AlN/GaN Recessed T-gated HEMT with Fe-doped Buffer for Future Power Electronic Applications. *NanoWorld J* 9(S5): S132-S136.

Abstract

GaN-HEMT (high-electron-mobility-transistor) power electronic applications require threshold voltage (V_{th}) controlling for safe operation. Electrical aspects including OFF-state leakage current, V_{th}, andforward operating current, all rely greatly on the work functionof the gate metal (ϕ_m). In this paper, we examined the influence of ϕ_m variation (the design factor that supports normally off operation) on the electrical properties of recessed T-gated AlN/GaN HEMT with AlGaN (Fe-doped) buffer. The simulationresults show that the highest gate metal (G_M) of 441.78 mS/mm, the peak I_D of 1.002 A/mm, and high f_T of 336.28 GHz is recorded for Mo-gate HEMT. As the values of ϕ_m are raised, then the V_{th} of the HEMT progressed in the right direction. This trend of V_{th} can be ascribed to the uplift of the conduction band (CB) in proportion to the increasing ϕ_m values. The findings imply thatgate-engineering can be used to produce depletion-mode (D-mode) and enhancement-mode (E-mode) AlN/GaN HEMTs at sub-100 nm regimes, enabling fail-safe future generation power electronics.

Keywords

AlN/GaN, T-gate, Fe-doping, Gate-engineering, Cut-off frequency, Threshold voltage

Introduction

With inherent superlative physical attributes, GaN-HEMTs exhibit exceptional microwave power characteristics and meet the requirements of high-speed performance [1-5]. Thus, GaN-HEMTs are being rapidly investigated due to their wide range of application domains such as commercial and military, radio astronomy, 5G/6G communications, photodetectors and laser diodes, SATCOM, sensors, RADARs, etc. [1-5]. The standard AlGaN/GaN (AG)-HEMTs have shown good RF, DC and power performance in recent years. To uplift the performance of RF GaN-HEMT, research communities have been exploring different techniques such as ultrathin barrier, sub-100 nm tapered gate, scaling down drain-to-source spacing (L_{SD}), T- gate technology, etc. Besides, gate length (L_G) and gate-to- channel space (d) must be optimized to avoid SCEs (short channel effects). GaN-HEMT with high Al-content ultrathin AlGaN barrier suffer from strain problems and are prone to SCEs at sub-micron Lg due to suboptimal L_G/d (aspect ratio) [5, 6]. Moreover, employing recessed gate approach to such devices is challenging, which predominantly causessubstantial gate leakage and aids reliability problems [1-5].Since the last few years, AlN/GaN HEMTs have drawnimmense research interest and as a result of rapid exploration, emerged as a promising technology with remarkable achievements in terms of RF, DC and power performance attributable to high carrier-density (n_s) of quantum-well (QW) because of wide energy-gap (E_g) (= 6.2 eV) and high polarization (piezoelectric + spontaneous) of AlN binary material. As scaling of L_G helps to outstretch operating frequency (f_T), the unavoidable SCEs always cast a shadow on this approach [5, 6]. On the other hand, including a back-barrier (BB) layer in the architecture of GaN-HEMT hasbecome a supreme choice that aids RF behavior, in addition to combating the SCEs. A binary (AlN), ternary (AlGaN, InGaN, AlInN, BGaN, Pdiamond, etc.) or quaternary (InAlGaN) alloy metals can be used as a BB [1-9]. Thedifference in E_g values of BB layer and GaN channel gives rise to CB offset at the BB/GaN junction aiding QW confinement. On the other hand, the number of charge carriers dispersing into the underlying buffer region will alsocome down due to the effective confinement [1-9].

Reliability problems due to self-heating, deep levels found at hetero-interfaces, and exposure to radiation, etc., can degrade the expected performance of GaN-HEMT. Because of the leftover impurities during the buffer growth process, leakage current rises and declines breakdown voltage (V_{br}) [1-13]. Besides, to capitalize on the material benefits of the HEMTs, a highly resistive buffer is necessary [10-13]. In this regard, the research community has adopted carbon (C) or iron (Fe) doping in the buffer layers [10-13]. The breakdown performance can also be improved with the help of Fe-doped buffer in the HEMT architecture [10-13].

Normally-ON (D-Mode) nature due to the presence of 2DEG limits the widespread of GaN-HEMTs since to ensure safe operation and durability, E-Mode operation is required which needs added circuitry to achieve OFF-condition, increasing the size of the device [14-17]. The V_{th} of GaN-HEMT can be engineered using techniques like gate-metallization, gate-recess, etc. Schottky-barrier-height (ϕ_b) varies for different gate metals, thus paving the way to control the V_{th} of the HEMT [14-17].

A recessed T-gated AlN/GaN HEMT including AlGaN (Fe-doped) buffer is designed and the performance evaluation against gate engineering is reported in this work using TCAD software. In section 2, the device's structural description is presented. In section 3, the RF/DC traits of the HEMT are compared among different gate metal designs. The conclusion of this simulation work is given in the last section (4).

Experimentation

Device structure

Figure 1 schematically depicts the cross-sectional view of the proposed design used in our work. Among the commonly used substrates, SiC (Silicon carbide) has become the most preferred wafer for GaN power electronic devices since it has the smallest thermal-expansion-coefficient i.e., 3.2%, and least lattice mismatch i.e., 4% with GaN. In addition, SiC wafers also exhibit high-thermal-conductivity (= 4.9 W/cm/K), improving the device's reliability [1-4, 18-20]. Due to these advantages, the proposed structure is built on a (5-μm) SiC wafer. The epitaxy is made of an AlN nucleationlayer measuring 200 nm, an AlGaN buffer layer of 1000 nm doped using 3 x 10^{20} cm^{-3} of Fe, a 100 nm AlGaN BB, a 50 nmthin GaN channel, an AlN top-barrier (6 nm) layer, and a Si_3N_4 passivation (3 nm) layer. Apart from length, the structure of

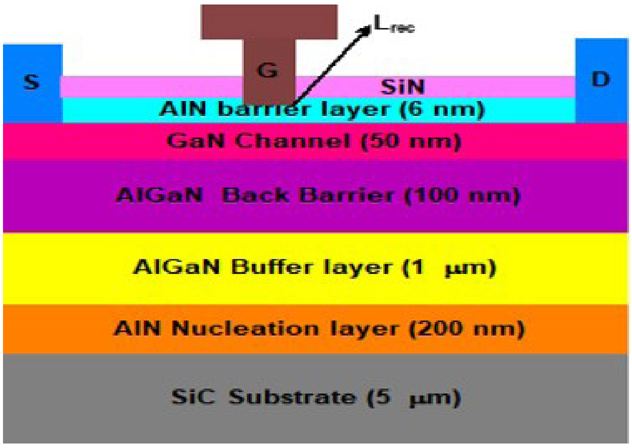

Figure 1: Structural illustration of proposed AlN/GaN HEMT.

the gate also influences the performance of the HEMT. Usinga T-shaped gate architecture is among the most prominent ways to improve electronic properties. In our design, the recessed T-gate features a 50 nm-wide footprint, a stem that is 75 nm tall, and a broad head measuring 250 nm. The gate- drain (L_{GD}) and gate-source (L_{GS}) separations are chosen as 500 nm and 250 nm, respectively. The gate has a fixed width (W_G) of 200 μm. The material parameters at 300 K and all the physical models adopted in this simulation can be found in [1]. Figure 2a and 2b depicts the TCAD simulation diagrams ofthe HEMT.

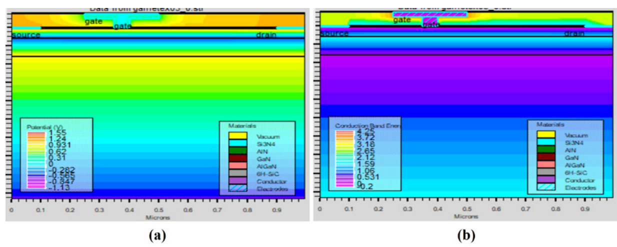

Figure 2: (a) Potential distribution of the simulated AlN/GaN HEMT and **(b)** CB energy distribution of the simulated AlN/GaN HEMT.

Results and Discussion

GaN-HEMTs entered the nanoelectronics regime to meet the continuous quest for improving RF performance. To overcome the physical and fundamental limitations of scaling down the transistor, GaN quantum-engineered HEMTs leverage on more innovative architectures, nanoengineered interfaces with minimal defects, design of confined quantum wells with nanoscale layers for efficient charge transport, incorporating gate structures with a nano-sized footprint, etc. [21-23]. The fabrication of GaN-HEMTs at the nanometer regime presents several significant challenges due to the inherently small dimensions and unique material properties of GaN. Achieving high material quality, precise control over nanoscale features, obtaining accurate doping profiles and concentrations are some of the key fabrication challenges that can be addressed by using epitaxial growth techniques such as MBE, MOCVD, PECVD, etc., advanced lithography techniques such as nanoimprint lithograph, optical-, UV-, and Deep UV lithography, etc., and the latest deposition and etching techniques [21-23]. Managing heat dissipation in nanoscale devices is another serious challenge and can result in thermal issues that affect device reliability. Adoption of SiC wafer helps to maintain lower operating temperatures, improve device reliability, and enhance the performance and efficiency of GaN HEMTs in high-frequency and high-power applications [1-4, 24-27].

The charge carriers in the QW of GaN HEMTs, whether they are D- or E- mode devices, are influenced by the Schottky gate. The electrical properties are governed by the ϕ_b between the G_M and the semiconductor lying below it. To investigate the relationship between ϕ_b and V_{th} shift, we haveselected five common gate metals, listed in table 1. The proposed HEMT is simulated using different gate metals and due to their ϕ_b difference, the V_{th} of the HEMT is shifted. By using the TCAD tool, we have examined the RF/DC characteristics of the designed gate-engineered structure in this work. The band structure diagram of the HEMT is depicted in figure 3 with varying values of ϕ_m.

Table 1: Work functions Φ_m (eV) for different G_M utilized in this work.

Metal	Φ_m (eV)
Al	4.3
Mo	4.6
Au	5.1
Ir	5.27
Pt	5.65

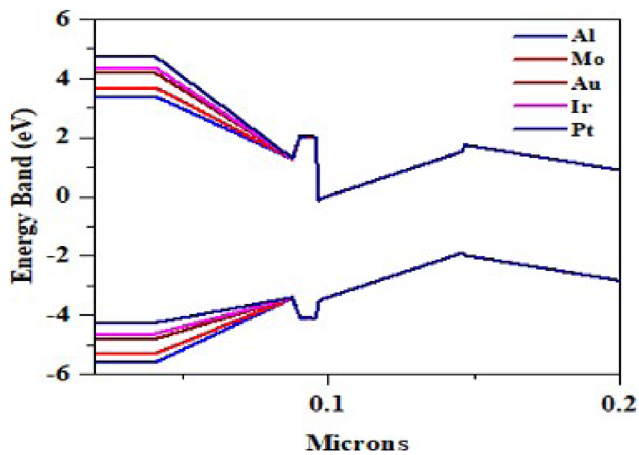

Figure 3: Energy-band (EB) diagram of the proposed AlN/GaN HEMTagainst varying values of ϕ_m.

Analysis of DC characteristics

Figure 4 and figure 5 depict the transconductance (G_M) curves and transfer characteristics of Al-, Mo-, Au-, Ir-, and Pt-gate HEMTs at V_{DS} = 1.4 V. The HEMT measured peak G_M values of 438.67 mS/mm for the Al-contact, 441.78 mS/mm for the Mo-contact, 438.24 mS/mm for the Au-contact, 438.52 mS/mm for the Ir-contact, and 438.4 mS/mm for the Pt-contact (Figure 4). The peak values of I_D obtained from the transfer curves shown in figure 5 are 0.999 A/mm, 1.002 A/mm, 0.988 A/mm, 0.982 A/mm, and 0.988 A/mm for Al-, Mo-, Au-, Ir-, and Pt-gated HEMTs, respectively. From the results, it is evident that the device displayed a +ve shift of V_{th} with raising ϕ_m values. This can be understood with the help of disparity in the EB diagram arising from various gate metal designs and theirrespective ϕ_b values (Figure 3). The simulated band-diagrams explore the impact of gate-engineering on the electrical properties of the HEMT are shown in figure 3. The fundamental factor contributing to the disparity in the EB diagram is the CB edge's uplift, that increases in direct proportion with rising ϕ_m values resulting from various Schottky-barrier-heights (ϕ_b) [14-17]. The AlN/GaN epitaxial n_S substantially decreases as ϕ_m values increase, which is reflected in an increase in V_{th}. Increasing ϕ_m values result in longer ϕ_b, which are evidenced by a positive shift of V_{th}.

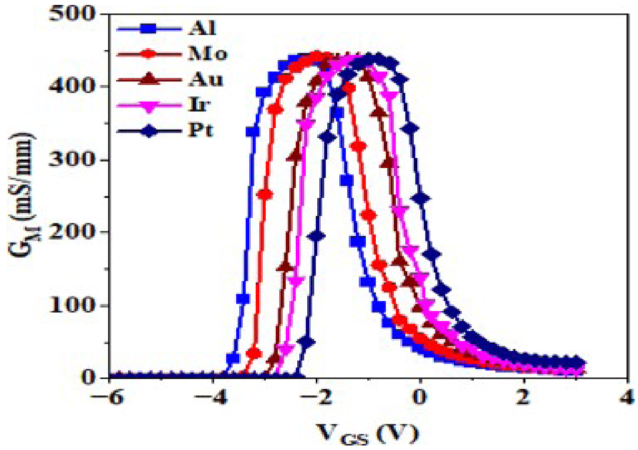

Figure 4: Transconductance curves of the proposed AlN/GaN HEMT againstvarying ϕ_m values.

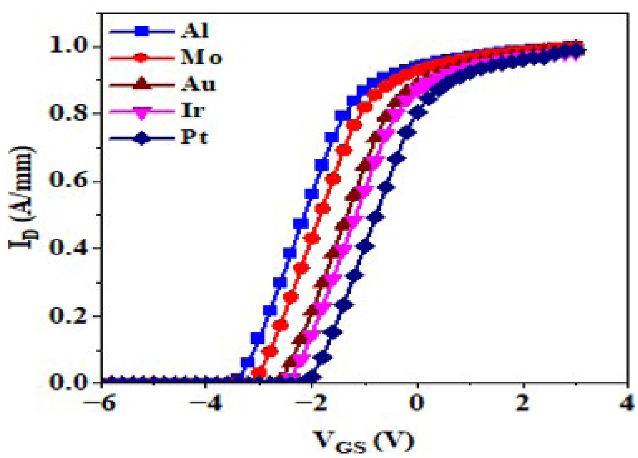

Figure 5: Transfer curves of the proposed AlN/GaN HEMT different ϕ_m values.

Analysis of RF characteristics

The RF traits of the structure were also examined to assess the relationship between V_{th} and the ϕ_b of various gate metals. The f_T-V_{GS} curves of the HEMT with various gate metals are depicted in figure 6. The f_T values extracted for Al-,Mo-, Au-, Ir-, and Pt-gated HEMTs are 335.1 GHz, 336.28 GHz, 336.53 GHz, 334.91 GHz, and 334.95 GHz, respectively. The RF outputs (Figure 6) reveal that the device shows a +ve shift of V_{th} with raising ϕ_m values. Capacitance measurement is performed to further confirm the V_{th} variation between

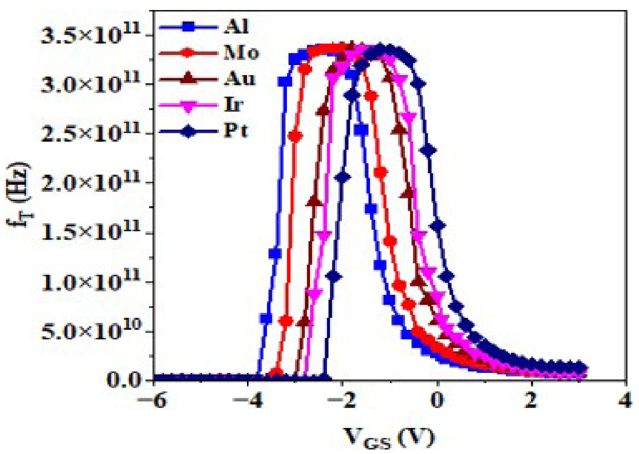

Figure 6: f_T vs V_{GS} curves of the proposed AlN/GaN HEMT against varying ϕ_m values.

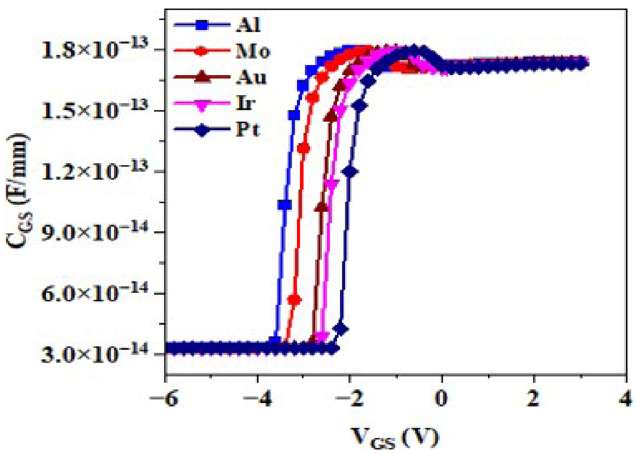

Figure 7: C_{GS} curves of the proposed AlN/GaN HEMT against varying ϕ_m values.

devices. Figure 7 and figure 8 depict the variationsof the gate-to-source (C_{GS}) and gate-to-drain (C_{GD}) capacitance at an applied V_{DS} of 1.4 V for different gate metal values. Based on the C-V plots (Figure 7 and figure 8), the HEMT with Al-, Mo-, Au-, Ir-, and Pt-gates produced the peak C_{GG} of 2.58 x 10^{-13} F/mm, 2.57 x 10^{-13} F/mm, 2.57 x 10^{-13} F/mm, 2.58 x 10^{-13} F/mm, and 2.57 x 10^{-13} F/mm @ V_{GS} = 3 V, respectively. The trend of the V_{th} shift against raising ϕ_m values is consistent inthe C-V curves of figure 7 and figure 8.

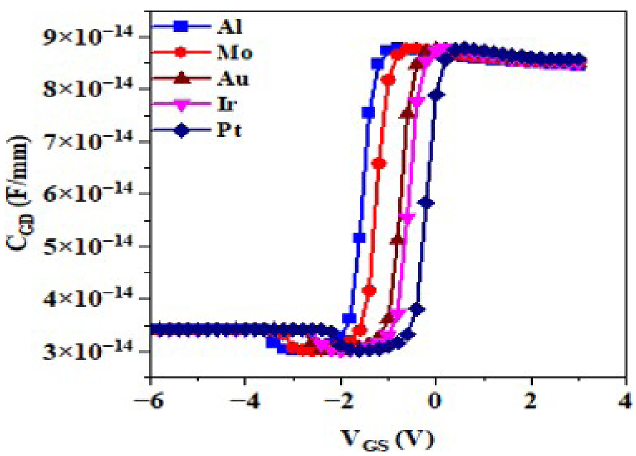

Figure 8: C_{GD} curves of the proposed AlN/GaN HEMT against varying ϕ_m values.

Conclusion

The electrical performance of AlN/GaN HEMT employing distinct gate metals was investigated in this work. It is observed that the CB edge of the HEMT exhibited an uplift in accordance with the increasing values of ϕ_m. This variation in the band diagram is ascribed to the variation of corresponding ϕ_b values. Better performance both in DC and RF domains is obtained for Mo-gate HEMT, while a near performance is observed in the remaining cases. Using varied gate metals in accordance with their various work functions, it was noticed that the HEMTs' threshold voltages shifted. The right shift of V_{th} is noticed with increasing ϕ_m values. The evidence of V_{th} shifts using gate engineering gives an alternative method to integrate E- and D-mode devices for thevertical and lateral scaling of GaN-HEMTs intended for high-frequency performance. In summary, T-gate-based AlN/GaNHEMT with Fe-doped buffer is an excellent device with effective confinement provided by BB and has great potential for next-generation RF power electronics at scaled gate lengths.

Acknowledgements

None.

Conflict of Interest

None.

References

1. Subramani NK, Sahoo AK, Nallatamby JC, Sommet R, Rolland N, et al. 2016. Characterization of parasitic resistances of AlN/GaN/AlGaN HEMTs through TCAD-based device simulations and on-wafer measurements. *IEEE Trans Microw Theory Tech* 64(5): 1351-1358. https://doi.org/10.1109/TMTT.2016.2549528
2. Chahdi HO, Benbakhti B, Mattalah M, Gerbedoen JC, Jaouad A, et al. 2020. Mechanisms of a rectifying TiN gate contact for AlGaN/GaN HEMTs on silicon substrate. *IEEE Trans Nanotechnol* 19: 682-688. https://doi.org/10.1109/TNANO.2020.3019916
3. Nagarajan V, Chen KM, Lin HY, Hu HH, Huang GW, et al. 2020. Low-frequency noise characterization of AlGaN/GaN HEMTs and MIS-HEMTs under UV illumination. *IEEE Trans Nanotechnol* 19: 405-409. https://doi.org/10.1109/TNANO.2020.2992732
4. Zhang H, Gan Y, Yang S, Sheng K, Wang P. 2021. Low limit of detection of the AlGaN/GaN-based sensor by the Kelvin connection detection technique. *Microsyst Nanoeng* 7(1): 51. https://doi.org/10.1038/s41378-021-00278-7
5. Harrouche K, Kabouche R, Okada E, Medjdoub F. 2019. High performance and highly robust AlN/GaN HEMTs for millimeter-wave operation. *IEEE J Electron Devices Soc* 7: 1145-1150. https://doi.org/10.1109/JEDS.2019.2952314

6. Hickman A, Chaudhuri R, Li L, Nomoto K, Bader SJ, et al. 2020. First RF power operation of AlN/GaN/AlN HEMTs with >3 A/mm and 3 W/mm at 10 GHz. *IEEE J Electron Devices Soc* 9: 121-124. https://doi.org/10.1109/JEDS.2020.3042050
7. Yang L, Hou B, Jia F, Zhang M, Wu M, et al. 2022. The DC performance and RF characteristics of GaN-based HEMTs improvement using graded AlGaN back barrier and Fe/C co-doped buffer. *IEEE Trans Electron Devices* 69(8): 4170-4174. https://doi.org/10.1109/TED.2022.3179675
8. Zhang Y, Teo KH, Palacios T. 2016. Beyond thermal management: incorporating p-diamond back-barriers and cap layers into AlGaN/GaN HEMTs. *IEEE Trans Electron Devices* 63(6): 2340-2345. https://doi.org/10.1109/TED.2016.2553136
9. Green AJ, Gillespie JK, Fitch RC, Walker DE, Lindquist M, et al. 2019. ScAlN/GaN high-electron-mobility transistors with 2.4-A/mm current density and 0.67-S/mm transconductance. *IEEE Electron Device Lett* 40(7): 1056-1059. https://doi.org/10.1109/LED.2019.2915555
10. Meneghini M, Rossetto I, Bisi D, Stocco A, Chini A et al. 2014. Buffer traps in Fe-doped AlGaN/GaN HEMTs: investigation of the physical properties based on pulsed and transient measurements. *IEEE Electron Device Lett* 61(12): 4070-4077. https://doi.org/10.1109/TED.2014.2364855
11. Ando Y, Makisako R, Takahashi H, Wakejima A, Suda J. 2021. Dependence of electrical characteristics on epitaxial layer structure of AlGaN/GaN HEMTs fabricated on freestanding GaN substrates. *IEEE Trans Electron Devices* 69(1): 88-95. https://doi.org/10.1109/TED.2021.3126270
12. Raja PV, Bouslama M, Sarkar S, Pandurang KR, Nallatamby JC, et al. 2020. Deep-level traps in AlGaN/GaN-and AlInN/GaN-based HEMTs with different buffer doping technologies. *IEEE Trans Electron Devices* 67(6): 2304-2310. https://doi.org/10.1109/TED.2020.2988439
13. Jia F, Ma X, Yang L, Hou B, Zhang M, et al. 2021. The influence of Fe doping tail in unintentionally doped GaN layer on DC and RF performance of AlGaN/GaN HEMTs. *IEEE Trans Electron Devices* 68(12): 6069-6075. https://doi.org/10.1109/TED.2021.3123113
14. Ge M, Li Y, Zhu Y, Chen D, Wang Z, et al. 2021. Effects of gate work function on E-mode AlGaN/GaN HEMTs with stack gate β-Ga_2O_3/p-GaN structure. *J Phys D Appl Phys* 54(35): 355103. https://doi.org/10.1088/1361-6463/ac0a0b
15. Guowang L, Zimmermann T, Cao Y, Chuanxin L, Xiu X, et al. 2010. Threshold voltage control in $Al_{0.72}Ga_{0.28}N$/AlN/GaN HEMTs by work-function engineering. *IEEE Electron Device Lett* 31: 954-956. https://doi.org/10.1109/LED.2010.2052912
16. Visvkarma AK, Sharma C, Laishram R, Kapoor S, Rawal DS, et al. 2019. Comparative study of Au and Ni/Au gated AlGaN/GaN high electron mobility transistors. *AIP Adv* 9(12): 125231. https://doi.org/10.1063/1.5116356
17. Lin HK, Huang FH, Yu HL. 2010. DC and RF characterization of AlGaN/GaN HEMTs with different gate recess depths. *Solid State Electron* 54(5): 582-585. https://doi.org/10.1016/j.sse.2010.02.001
18. Du H, Zhang J, Zhou H, Liu Z, Zhang T, et al. 2022. GaN high-electron-mobility-transistor on free-standing GaN substrate with low contact resistance and state-of-the-art f_T x L_G value. *IEEE Trans Electron Devices* 69(3): 968-972. https://doi.org/10.1109/TED.2021.3138954
19. Ozaki S, Yaita J, Yamada A, Kumazaki Y, Minoura Y, et al. 2021. First demonstration of X-band AlGaN/GaN high electron mobility transistors using free-standing AlN substrate over 15 W mm^{-1} output power density. *Appl Phys Express* 14(4): 041004. https://doi.org/10.35848/1882-0786/abec90
20. Cui P, Zeng Y. 2021. Electrical properties of 90-nm InAlN/GaN HEMT on silicon substrate. *Phys E Low Dimens Syst Nanostruct* 134: 114821. https://doi.org/10.1016/j.physe.2021.114821
21. Niranjan S, Muralidharan R, Sen P, Nath DN. 2022. Au-Free AlGaN/GaN HEMT on flexible kapton substrate. *IEEE Trans Electron Devices* 69(8): 4212-4217. https://doi.org/10.1109/TED.2022.3186267
22. Mishra S, Kachhawa P, Mondal P, Ghosh S, Tripura C, et al. 2022. AlGaN/GaN HEMT based biosensor for detection of the HER2 antigen spiked in human serum. *IEEE Trans Electron Devices* 69(8): 4527-4533. https://doi.org/10.1109/TED.2022.3184658
23. Joshi V, Soni A, Tiwari SP, Shrivastava M. 2016. A comprehensive computational modeling approach for AlGaN/GaN HEMTs. *IEEE Trans Nanotechnol* 15(6): 947-955. https://doi.org/10.1109/TNANO.2016.2615645
24. Kumar A, Capua E, Fontanesi C, Carmieli R, Naaman R. 2018. Injection of spin-polarized electrons into a AlGaN/GaN device from an electrochemical cell: evidence for an extremely long spin lifetime. *ACS Nano* 12(4): 3892-3897. https://doi.org/10.1021/acsnano.8b01347
25. Zhu J, Zhou X, Jing L, Hua Q, Hu W, et al. 2019. piezotronic effect modulated flexible AlGaN/GaN high-electron-mobility transistors. *ACS Nano* 13(11): 13161-13168. https://doi.org/10.1021/acsnano.9b05999
26. Merazga S, Keffous A, Brighet A, Kechouane M. 2017. Effect of thermal annealing on the optical and structural Properties of the a-SiC thin films deposited by DC magnetron sputtering. *NanoWorld J* 3(3): 54-58. https://doi.org/10.17756/nwj.2017-047
27. Gangopadhyay P. 2018. Metallic alloy nanoparticles and metal-semiconductor nanomaterials. *NanoWorld J* 4(3): 31-42. https://doi.org/10.17756/nwj.2018-058